

1 **Performance and kinetic modelling of photolytic and**
2 **photocatalytic ozonation for enhanced micropollutants removal**
3 **in municipal wastewaters**

4

5 Danilo Bertagna Silva, Alberto Cruz-Alcalde, Carmen Sans, Jaime Giménez*, Santiago
6 Esplugas

7 Department of Chemical Engineering and Analytical Chemistry, Faculty of Chemistry,
8 Universitat de Barcelona, C/Martí i Franqués 1, 08028 Barcelona, Spain

9

10 *Corresponding Author: Jaime Gimenez, j.gimenez@ub.edu

11

12 **ABSTRACT**

13 In this work, the performances of ozonation, photolytic ozonation (UV-C/O₃), and
14 photocatalytic ozonation (UV-A/TiO₂/O₃) in degrading ozone recalcitrant
15 micropollutants in four different real domestic wastewaters were evaluated in semi-
16 continuous operation, together with the influence of water matrices in the ozone mass
17 transfer and pollutant degradation rates. The •OH exposure per consumed ozone ratio,
18 defined as R_{OH,O₃}, was applied for single ozonation and modified for light-assisted
19 ozonation processes to evaluate and compare the contribution of radical pathway on
20 micropollutants abatement for the different wastewaters studied. R_{OH,O₃} plots presented
21 good fitting ($R^2 > 0.95$) in two stages, corresponding to different ozone mass transfer
22 regimes, for all cases. Light-assisted ozonation attained higher pollutant degradation for

23 all water matrices compared to single ozonation, although the performance of UV-
24 assisted processes was more sensitive to matrix factors like composition and turbidity.
25 Moreover, the improvement brought by both light-based processes on R_{OHO_3} values
26 mainly took place during the second stage. Thus, photocatalytic ozonation reached R_{OHO_3}
27 values higher than double for all wastewaters, compared with single ozonation (between
28 105% and 127% increase). These values represent a saving of almost half of the overall
29 ozone needs (42%) for the same ozone recalcitrant micropollutant depletion, although it
30 would require the adoption of higher ozone doses than the currently employed for
31 ozonation in wastewater treatment plants.

32

33 **KEYWORDS**

34 Wastewater ozonation; UV light; photocatalysis; advanced oxidation processes;
35 recalcitrant micropollutants.

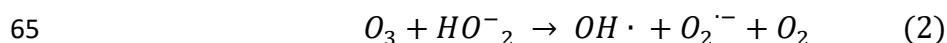
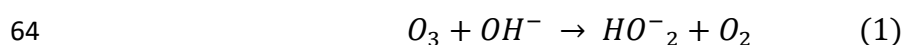
36

37 **1. Introduction**

38 The ever-growing development, production and consumption of new chemical
39 substances have raised the need of developing new technologies for wastewater treatment
40 because many of these substances show a bio-accumulative and non-biodegradable
41 character, persisting in the environment [1]. These substances are commonly called
42 micropollutants (MP) because their presence on water bodies and wastewater treatment
43 plants (WWTP) effluents ranges from nano (ng L^{-1}) to micro ($\mu\text{g L}^{-1}$) scale [2, 3]. Their
44 presence in the aquatic environment is associated to a variety of negative effects,
45 including short and long-term toxicity, endocrine disruption and antibiotic resistance in
46 microorganisms [4,5].

47 The high oxidation potential of ozone (O₃) makes it an effective tool for
 48 wastewater treatment, with demonstrated performance by many studies from laboratory
 49 to full scale [6, 7, 8]. The quick decomposition of ozone leaves no traces of its presence
 50 in water, unlike chlorine. However, ozone is a selective oxidant. Second-order rate
 51 constants for ozone vary several orders of magnitude, between < 0.1 M s⁻¹ and 7x10⁹ M
 52 s⁻¹ [9]. Due to its high production costs, ozone doses typically employed are relatively
 53 low: TOD/DOC (transferred ozone dose/dissolved organic carbon) ratios range between
 54 0.5 and 1.5 [10].

55 The stress caused by global water scarcity has been increasing demands of
 56 wastewater reuse for direct human consumption [11]. Therefore, higher purity standards
 57 have to be attained to eliminate all pollutants and allow a safe use of water. Higher O₃
 58 doses can be a way of reaching this goal, because the natural decomposition of ozone
 59 generates hydroxyl radicals (•OH) in non-acidic pHs (equations 1 and 2). These radicals
 60 have a higher oxidation potential than ozone and they are non-selective oxidants, being
 61 able to oxidize many molecules that ozone cannot. Therefore, this is an interesting option
 62 for the abatement of recalcitrant micropollutants and attain a high level of water purity
 63 [12].

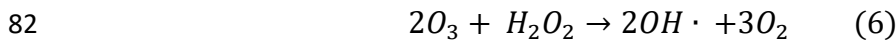
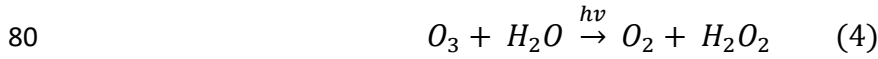


66 Degradation of a micropollutant during ozonation can be described by equation 3,
 67 accounting for the sum of molecular ozone and hydroxyl radicals contribution [13]. There
 68 is a considerable number of data on kinetic constants of pollutants reactions with
 69 molecular ozone and the hydroxyl radical [14, 15], being those for hydroxyl radical in the
 70 range of 10⁹ – 10¹⁰ M s⁻¹ for most of micropollutants.

$$-\ln\left(\frac{[MP]}{[MP]_0}\right) = k_{MP,O_3} \int [O_3] dt + k_{MP,OH\cdot} \int [OH\cdot] dt \quad (3)$$

Ultra-violet light is commonly adopted on wastewater treatment plants for disinfection [16]. Many pollutants and cell membranes of microorganisms undergo photolysis. Their degradation rates vary with light intensity and wavelength, matrix composition and geometry of the reactor [17].

Ozone absorbs light at UV-C range, presenting a peak value at wavelength of 254 nm [12]. Equations 4-6 show the formation of hydroxyl radicals under these circumstances [18], creating a highly oxidative medium in a process called photolytic ozonation.



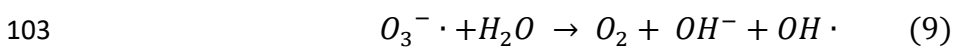
Besides contributing on radical formation, when UV light is included in the system, a first-order degradation rate photolysis of a target micropollutant should be accounted on the equation describing its abatement [18] (Eq. 7).

$$-\ln\left(\frac{[MP]}{[MP]_0}\right) = k_{MP,O_3} \int [O_3] dt + k_{MP,OH\cdot} \int [OH\cdot] dt + k_{MP,UV} \int dt \quad (7)$$

The high photocatalytic activity of TiO₂ and some of its properties (economical, non-toxic, insoluble and stable in water [19]) make it a substance of great interest for wastewater treatment and recalcitrant pollutants abatement. With a band gap between 3.0 and 3.2 eV (UV-A, near visible), electrons on its valence band (e_{vb}⁻) can be promoted to conduction band (e_{cb}⁻), generating a reactive electron-hole pair when irradiated by UV light [20]. This pair can go back to its original place or engage in oxidation reactions with

93 the surrounding medium. In wastewater matrices, this can generate hydroxyl radicals and
94 contribute to micropollutants abatement [21, 22].

95 Ozonation and photocatalysis can be combined to attain a higher degree of
96 pollutant degradation in a process called photocatalytic ozonation. Ozone reacts with the
97 conductive-band electron, thus preventing its return to the valence band, and forms
98 ozonide radicals ($O_3^{\cdot -}$), an initial step towards the formation of more hydroxyl radicals
99 in this system, shown by equations 8 and 9 [23, 24, 25]. The degradation efficiency of
100 photocatalytic ozonation has been demonstrated in many lab-scale studies [26, 27, 28, 29,
101 30], but few of them have been performed on real wastewaters [31, 32].



104 The control of micropollutants removal and the optimization of the required ozone
105 dose during the process are still unaccomplished challenges. One of the most common
106 difficulties is the impossibility of directly measuring the hydroxyl radical concentration,
107 due to its nearly instantaneous reaction rates [33, 34]. Attempts to work around this
108 problem were made by the development of the recent $R_{OH\cdot O_3}$ concept, which is a valuable
109 step towards the prediction of pollutant abatement in ozonation processes [35]. The $R_{OH\cdot O_3}$
110 concept is defined as the hydroxyl radical exposure per transferred ozone dosage
111 (equation 10).

$$112 \quad R_{OH\cdot O_3} = \frac{\int [OH\cdot] dt}{TOD_t} \quad (10)$$

113 The $\bullet OH$ exposure can be obtained through the monitoring of a probe compound
114 with $k_{MP, O_3} < 10 \text{ M}^{-1} \text{ s}^{-1}$ [37]. For those ozone-resistant substances, substituting equation

115 10 on equation 7 results in equation 11, that can be used to predict pollutant degradation
116 [36]:

$$117 \quad -\ln\left(\frac{[MP]_t}{[MP]_0}\right) = k_{MP,OH} \cdot R_{OH,O_3} \cdot TOD_t \quad (11)$$

118 The goals of this study were: 1) to compare the performance of single, photolytic
119 and photocatalytic removal of ozone-resistant micropollutants in real municipal
120 wastewaters coming from different sources and processes, thus having very different
121 compositions; 2) to adapt and check the utility of the R_{OH,O_3} concept in the modelling of
122 these ozone-based processes; 3) to evaluate the influence of light and catalyst on the
123 ozonation of different real domestic wastewaters through the R_{OH,O_3} parameter.

124

125 **2. Materials and Methods**

126 *2.1 Chemical and reagents*

127 Acetamiprid (ACMP) and atrazine (ATZ) analytical standards were acquired from
128 Sigma-Aldrich (Germany). Ultrapure water was produced in site by a filtration system
129 (Millipore, USA). Pure oxygen ($\geq 99.99\%$) was supplied by Abelló Linde (Spain).
130 Titanium Dioxide P-25 was supplied by Evonik (primary particle size of 21 nm).

131 *2.2 Wastewater characterization*

132 Four wastewater effluents were employed in this work from two different WWTPs
133 in Gavà and El Prat (Barcelona, Spain). Two of them came from Gavà station (MBR –
134 outlet of a membrane bioreactor, MBBR – outlet of a moving bed biofilm reactor) and
135 the other two came from El Prat station (CAS – conventional activated sludge, CAS-DN
136 - conventional activated sludge with denitrification). Their main quality parameters are

137 gathered in Table 1. (TOC: total organic carbon; COD: chemical oxygen demand; UV₂₅₄:
 138 specific absorbance at 254 nm) All the effluent samples were filtered with conventional
 139 filter paper, to remove coarse particles, and stored at 4 °C prior to use.

140

141 Table 1. Effluent characterization

Wastewater ID	pH	Turbidity [NTU]	TOC [mg C L ⁻¹]	COD [mg O ₂ L ⁻¹]	UV ₂₅₄ [m ⁻¹]	DOC [mg C L ⁻¹]	Alkalinity [mg CaCO ₃ L ⁻¹]
MBR	7.7	0.5	13.6	14.9	17.4	13.3	208
CAS-DN	7.5	2.6	13.2	27.3	24.6	13.4	275
CAS	8.0	20.1	37.8	70.5	48.9	18.7	449
MBBR	7.8	18.5	51.1	71.3	50.3	21.7	469

142

143 *2.3 Single and light assisted ozonation experiments*

144 Ozone was produced from pure oxygen by a 301.19 lab ozonizer (Sander,
 145 Germany). The ozonation of wastewaters was performed in a 1.5 L jacketed reactor
 146 covered with aluminum foil, to avoid radiation losses, and operated in semi-continuous
 147 mode. Ozone was injected at the bottom of the reactor by a porous diffuser. A magnetic
 148 stirrer ensured the good contact between liquid and gas phases and a homogeneous liquid
 149 phase. Experiments were performed at 22 ± 2 °C. The gas flow rate was maintained at 0.3
 150 L min⁻¹ and the inlet concentration of ozone at 10 mg L⁻¹ (values at STP conditions). Gas-
 151 phase ozone concentrations were continuously monitored by two BMT 964 ozone
 152 analyzers (BMT Messtechnik, Germany) placed on the reactor inlet and outlet. The ozone
 153 concentration in the liquid phase was measured by a Q45H/64 dissolved O₃ probe
 154 (Analytical Technology, USA), which was connected to a liquid recirculation stream. For
 155 experiments with TiO₂, the dissolved ozone was not measured to preserve the
 156 equipment's probe membranes from small solid particles.

157 A detailed scheme of the ozonation setup is shown elsewhere [36].

158 For experiments assisted by UV radiation, two different reactor configurations
159 were employed. In experiments with UV-C radiation, a single lamp (4W, 254 nm,
160 Phillips) with a photon fluence rate of 1.01 mW cm^{-2} (obtained by atrazine's actinometry
161 [37]) was used. For experiments with UV-A light, three black light bulb (BLB) lamps
162 (Philips TL 8 W-08 FAM) of 8 W each with a wavelength range 350-400 nm (maximum
163 at 365 nm) and a fluence rate of 5.47 mW cm^{-2} were used instead. In both cases, the lamps
164 –protected by means of quartz sleeves– were immersed and placed at the center of the
165 reaction vessel. Prior to start experiments, they were turned on for 20 minutes to attain a
166 constant photon flow.

167 For experiments using titanium dioxide, its addition to the reaction medium was
168 made at the concentration of 0.1 g L^{-1} . A magnetic stirrer homogenized the system for 20
169 minutes prior to the beginning of treatment.

170 The transferred ozone dose (TOD), which represents the accumulated amount of
171 ozone that is transferred to reactor per unit of volume during a given time, was
172 determined as explained in supplementary information (Text S1) [38].

173 All experiments ran for one hour. ACMP was used as $\bullet\text{OH}$ probe compound, since
174 it is an O_3 -resistant micropollutant ($k_{ACMP, \text{O}_3} = 0.25 \text{ M}^{-1} \text{ s}^{-1}$ and $k_{ACMP, \bullet\text{OH}} = 2.1 \cdot 10^9 \text{ M}^{-1} \text{ s}^{-1}$)
175 [39]. The spiked concentration of ACMP in all effluents was $100 \mu\text{g L}^{-1}$. Samples were
176 withdrawn at known time intervals and kept at room conditions until complete
177 consumption of dissolved ozone was achieved.

178 On each sample, the residual concentration of ACMP was measured by HPLC-
179 UV [39]. Prior to the analysis, samples were filtered using $0.45 \mu\text{m}$ PVDF syringe filters.

180 All different ozonation processes and the corresponding blank experiments were
181 also performed on Milli-Q water buffered with a pH 7 phosphate solution (1 M). The
182 results can be found on the Supplementary Information, Figs. S1 and S2.

183

184 **3. Results and discussion**

185 *3.1 Ozone mass transfer and ozone demand*

186 Ozone mass balance and demand could be assessed through continuously
187 monitoring inlet and outlet (gas phase) ozone concentrations, as well as dissolved (liquid
188 phase) ozone (Figs. S3-S7). Clearly, two kinetic regimes could be discerned: initially,
189 ozone mass transfer was very fast, attaining a η_{tr} value (slope of transferred versus applied
190 ozone doses plot) above 0.8 for all matrices and processes (see Table 2 and Fig. S8 on the
191 SI). During the first stage, all wastewaters contained substances that are highly reactive
192 with ozone, consuming it faster. In the second stage, encompassing the last 30 minutes
193 of experiment, the transfer yield decreased because it got controlled by moderate or slow
194 ozone rate reactions [12] and it was possible to discern the influence of different matrices:
195 wastewaters with a higher organic and inorganic carbon content (CAS and MBBR) had
196 higher ozone transfer yields.

197 When UV-C light was turned on, the η_{tr} value increased for all wastewaters in the
198 second stage. UV-C light accelerates ozone depletion (equation 4) leading to less ozone
199 leaving the system, thus optimizing the transfer yield for all cases. Ozone transfer yield
200 increase was higher for less turbid matrices, Milli-Q, MBR and CAS-DN, due to the better
201 UV-C radiation transmission on these media.

202 When UV-A was added to TiO₂ experiments, ozone mass transfer of the Milli-Q,
203 MBR and CAS-DN matrices improved considerably. Less turbidity and lower organic

204 matter content (see table 1) allowed more photon absorption by TiO₂, leading to a higher
 205 e⁻_{cb} production. Equation 8 shows how this may lead to additional ozone consumption in
 206 the system.

207 Table 2 also includes the instantaneous ozone demand (IOD) and the pseudo-first
 208 order decay rate of ozone (k_d) values obtained for ozonation (for definition and calculation
 209 methods see Text S1). Values for photolytic ozonation were not obtained because no
 210 ozone was detected in the liquid phase during those experiments due to the efficient ozone
 211 decomposition under those integrated systems. IOD describes the ozone demand when it
 212 is instantaneously consumed by the wastewater, and consequently represents the dose of
 213 ozone at the point of the transition between primary (fast) and secondary (slow) ozonation
 214 stages [38]. As it is expected, more polluted matrices had higher IODs. For real
 215 wastewaters, an IOD/DOC ratio of approximately 1.0 ± 0.1 was obtained for all
 216 wastewaters tested. Milli-Q water presented two phases and IOD value of 4 mg/L due to
 217 the ACMP addition.

218 k_d values were higher for more polluted water, but since the TOC value of MBR
 219 and CAS-DN are similar, the latter had a slower O₃ decomposition due to its higher
 220 alkalinity content [40].

221

222

223 Table 2: O₃ mass transfer, IOD and k_d for all studied waters. All R² > 0.99

Process	MATRIX ID	η _{tr} [trans. O ₃ /app. O ₃]		IOD [mgO ₃ L ⁻¹]	k _d [min ⁻¹]
		Stage 1	Stage 2		
Ozonation	Milli-Q	0.86	0.14	4	0.10
UV-C/O ₃		0.90	0.40	-	-
TiO ₂ /O ₃		0.89	0.04		
TiO ₂ /UV-A/O ₃		0.87	0.40		
Ozonation	MBR	0.82	0.17	12	0.14

UV-C/O ₃		0.82	0.37	-	-
TiO ₂ /O ₃		0.87	0.14		
TiO ₂ /UV-A/O ₃		0.83	0.35		
Ozonation		0.88	0.17	15	0.05
UV-C/O ₃	CAS-DN	0.91	0.41	-	-
TiO ₂ /O ₃		0.82	0.20		
TiO ₂ /UV-A/O ₃		0.80	0.29		
Ozonation		0.85	0.30	18	0.29
UV-C/O ₃	CAS	0.89	0.44	-	-
TiO ₂ /O ₃		0.88	0.27		
TiO ₂ /UV-A/O ₃		0.83	0.30		
Ozonation		0.88	0.31	25	0.54
UV-C/O ₃	MBBR	0.94	0.37	-	-
TiO ₂ /O ₃		0.95	0.27		
TiO ₂ /UV-A/O ₃		0.85	0.28		

224

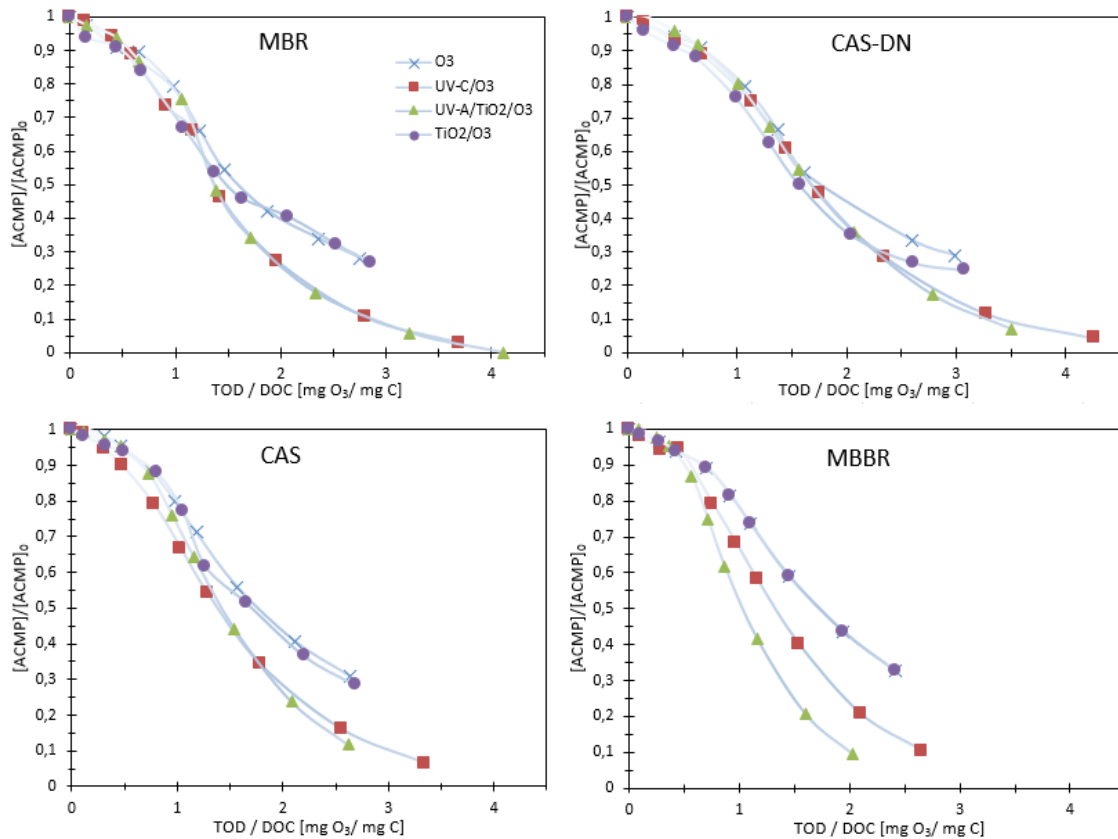
225 3.2 Degradation of a model O₃-resistant compound: ACMP

226 First of all, control tests for UV-A and UV-C photolysis and UV-A/TiO₂
 227 photocatalysis were performed to verify their contribution on photocatalytic ozonation.
 228 ACMP did not show any degradation due to UV-A photolysis, and UV-A/TiO₂
 229 photocatalysis presented little degradation for the MBR effluent sample (less than 6%)
 230 and no degradation for all the other wastewaters (figure S9 of the supplementary
 231 information). ACMP degradation by UV-C radiation ranked from 45% for MBBR up to
 232 60 % for MBR, increasing with the decrease of organic matter content and turbidity of
 233 wastewater (Figure S10).

234 Figure 1 shows degradation of ACMP for single, photolytic (UV-C),
 235 photocatalytic (UV-A/TiO₂) and catalytic (TiO₂) ozonation in all matrices tested, at
 236 different TOD/DOC ratios. Figure S11 shows the same degradation per reaction time (60
 237 minutes).

238 TiO₂/O₃ did not bring any clear improvement with respect to single ozonation.
 239 However, photo-assisted processes significantly improved the abatement of ACMP,

240 demonstrating the enhanced $\bullet\text{OH}$ production. Photolytic ozonation showed final ACMP
 241 degradations above 90% for all matrices. Photocatalytic ozonation was the most matrix-
 242 influenced process: MBR matrix reached 100% of ACMP final degradation – being the
 243 highest of all the experiments – but this value dropped on each of the other matrices: final
 244 degradation in CAS-DN was 93% and in CAS and MBBR, 89%. As more organic matter
 245 adsorbed on the catalyst surface hinders its photo-activity, photocatalytic ozonation
 246 efficiency decreases. Moreover, turbid matrices also hinder photo-activity, as well as the
 247 presence of dissolved UV-absorbent organic species, thus decreasing the amount of
 248 photons reaching the catalyst surface.



249

250 Figure 1. ACMP degradation per TOD/DOC_0 ratio for all studied wastewaters. Gas flow rate = 0.3 L
 251 min^{-1} ; Inlet (g) ozone concentration = $10 \text{ mg O}_3 \text{ L}^{-1}$; $T_{\text{reaction}} = 20 \pm 2 \text{ }^\circ\text{C}$; $T_{\text{in}} (\text{gas}) = 22 \pm 2 \text{ }^\circ\text{C}$; $P_{\text{in}} (\text{gas}) =$
 252 $25 \pm 2 \text{ mbar}$.

253 On figure 1 it is possible to see that the two light-based ozonation processes started
254 to improve its effectiveness compared with single ozonation or TiO_2/O_3 at different
255 TOD/COD values. The cleaner matrices MBR and CAS-DN required a TOD/DOC ratio
256 of about 1.5, much higher than currently employed ratios for these types of waters (from
257 0.5 up to 1). This can be related to the two-stage character of the process: initially,
258 reactivity between O_3 and matrix compounds is very high, hindering radical production
259 with or without light. During second stage, quick O_3 reactions are less prominent and
260 radical formation paths are favored. Moreover, a decrease in turbidity during ozonation
261 would have allowed more photons to reach O_3 or TiO_2 molecules, promoting the radical
262 pathway as well. This means that, in order to improve ozone-resistant micropollutants
263 removal by light assisted processes, the employed ozone doses should also increase. In
264 return, the ozone doses required to reach satisfactory degradation levels of recalcitrant
265 micropollutants will be reduced due to the increase of $\bullet\text{OH}$ -exposure provided by light
266 assisted processes compared to single ozonation. In the case of ACMP, for 65% of initial
267 concentration removal, the needed TOD/DOC ratio decreased from 2.3 to 1.7 for MBR
268 and from 2.4 to 2.0 for CAS-DN, and consequently the corresponding ozone dose demand
269 for both light assisted processes would be lower (27% and 17%, respectively).

270 The addition of UV-C light and UV-A/ TiO_2 in the more polluted waters CAS and
271 MBBR clearly improved the overall AMCP degradation efficiency from lower
272 TOD/DOC ratios of 1.2 and 0.6, respectively. That is, improvement of $\bullet\text{OH}$ -exposure
273 provided by light assisted processes were assessed at TOD/COD ratios closer to currently
274 employed ones. Still, due to high organic content and alkalinity of these types of
275 wastewaters, the TOD/DOC needed for recalcitrant micropollutants abatement and
276 consequently the required ozone doses would be much higher. Thus, in the case of 65%
277 removal achievement of initial ACMP concentration, the TOD/COD ratio decreased from

278 2.2 in single ozonation to 1.7 for light assisted processes in CAS effluent, while for
279 MBBR wastewater, this ratio dropped from 2.4 down to 1.7 for photolysis and to 1.3 for
280 photocatalytic ozonation. The latter represents a saving of almost half of the overall
281 ozone needs (42%) for the same micropollutant degree of depletion.

282

283 3.3 R_{OH_3} determination

284 In this work, the recalcitrant pesticide acetamiprid was used as model compound
285 for R_{OH_3} estimation during wastewater ozonation. UV-C photolysis blank tests were
286 carried out for all wastewaters to quantify their contribution on ACMP degradation during
287 photolytic ozonation (equation 7). The first-order degradation rate $k_{MP,UV}$ obtained for
288 each matrix was used to deduct the amount of hydroxyl radical exposure at each reaction
289 time t , according to equation 12. During ozonation the matrices undergo several changes,
290 and it can be a source of error on degradation rate determination [12]. Being so, it is not
291 possible to determine separately how much of acetamiprid degradation is due to direct
292 photolysis and how much to the oxidation by the hydroxyl radical. Thus, factors affecting
293 photolysis were considered constant for all experiments and included in the $k_{MP,UV}$ value.

294

$$295 \int [OH \cdot] dt = \frac{\ln \left(\frac{[MP]_t}{[MP]_0} \right) + k_{MP,UV} * t}{-k_{MP,OH}} \quad (12)$$

296 Data of $\bullet OH$ exposure per consumed ozone dose fitted to linear model according
297 to equation 10 ($R^2 > 0.95$), obtaining R_{OH_3} values for all water matrices. These are shown
298 on table 3, and their plots are given on figure 2.

299

300 Table 3. $R_{\text{OH}\cdot\text{O}_3}$ values for plots on figure 2 and TOD to 65% of ACMP degradation. All $R^2 > 0.95$

Process	WASTEWATER ID	$R_{\text{OH}\cdot\text{O}_3}$ [10^7 s^{-1}]		TOD _{ACMP 65%} [$\text{mg O}_3 \text{ L}^{-1}$]
		S1	S2	
Ozonation	MBR	3.9	8.9	30
UV-C/ O_3		1.6	16.0	22
TiO_2/O_3		4.1	9.0	31
UV-A/ TiO_2/O_3		5.1	19.7	22
Ozonation	CAS-DN	2.5	8.5	34
UV-C/ O_3		1.6	12.8	28
TiO_2/O_3		3.4	9.1	29
UV-A/ TiO_2/O_3		4.5	17.4	28
Ozonation	CAS	2.4	7.0	45
UV-C/ O_3		1.7	9.6	33
TiO_2/O_3		1.5	7.2	43
UV-A/ TiO_2/O_3		1.4	14.3	33
Ozonation	MBBR	1.7	6.5	50
UV-C/ O_3		1.2	9.3	35
TiO_2/O_3		0.8	7.2	53
UV-A/ TiO_2/O_3		1.8	14.8	29

301

302 Two different ozonation regimes –stage 1 (S1) and stage 2 (S2)- were observed
 303 for all tests, corresponding to the two ozone transfer rates previously observed, and two
 304 $R_{\text{OH}\cdot\text{O}_3}$ values were fitted for each stage. Stage 2 values were higher than stage 1 for all
 305 cases. In stage 2, the slower molecular ozone consumption by the matrix allows more
 306 radical formation per transferred ozone by the different mechanism involved in the
 307 processes, increasing the $R_{\text{OH}\cdot\text{O}_3}$, as previously discussed.

308 By comparing $R_{\text{OH}\cdot\text{O}_3}$ it was possible to verify the matrix influence on radical
 309 production: waters with higher alkalinity and organic carbon content had smaller $R_{\text{OH}\cdot\text{O}_3}$
 310 values because many organic substances, bicarbonates and carbonates ions are well
 311 known radical scavengers [41, 42].

312 Comparing the $R_{\text{OH}\cdot\text{O}_3}$ values obtained for single and photolytic ozonation, the
 313 latter presented smaller values for stage 1 for all matrices. This can be explained by the
 314 hypothesis of a too low concentration of the peroxide generated intermediate. On stage 1

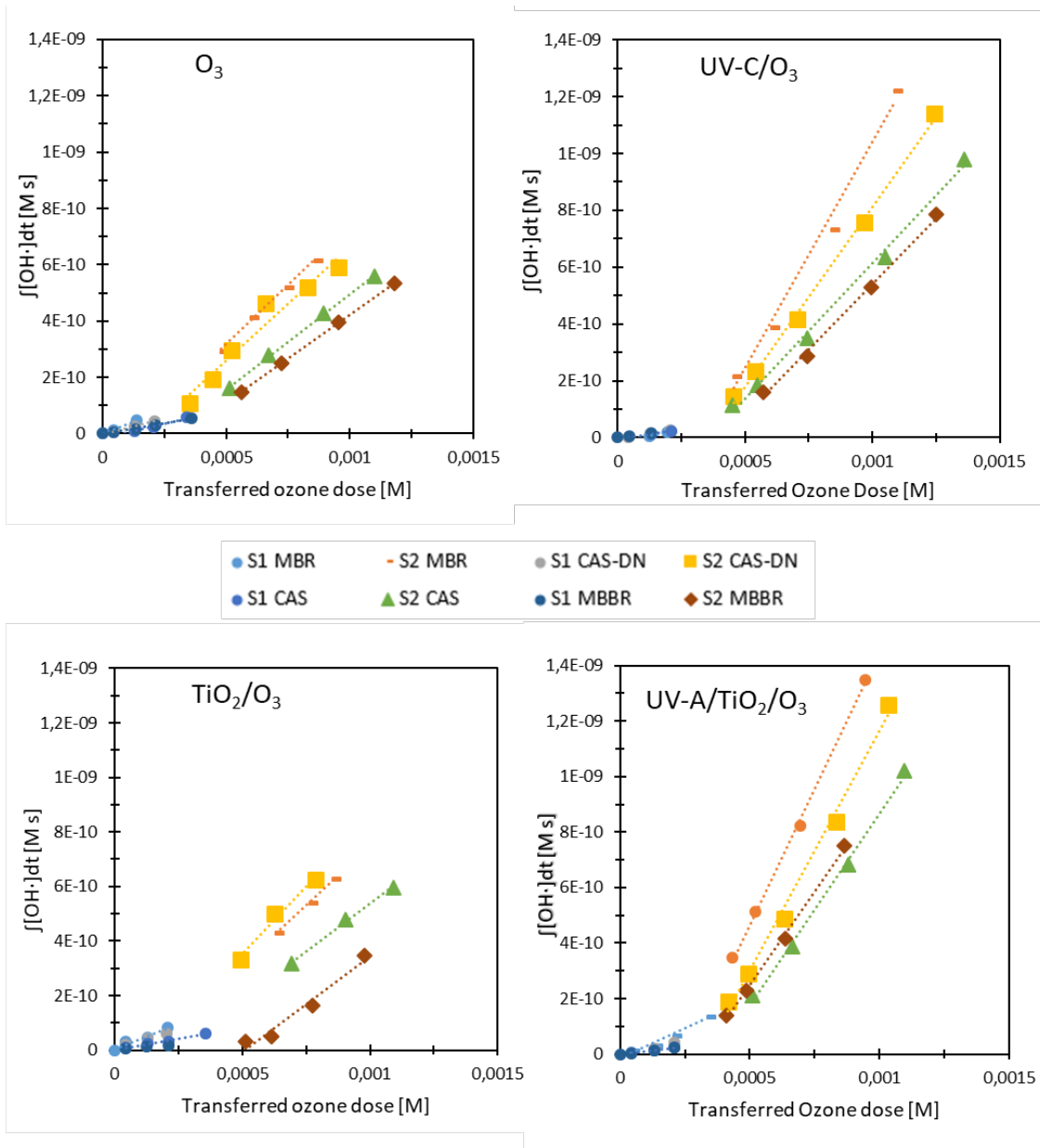
315 only a small amount of ozone is available for photolysis due to its quick reactivity with
316 the medium, generating a small amount of peroxide (equation 4). While ozone has a high
317 absorptivity at 254 nm in both liquid ($3300 \text{ M}^{-1}\text{cm}^{-1}$) and gas ($2950 \text{ M}^{-1}\text{cm}^{-1}$) phases [12],
318 peroxide absorbs at a much lower rate ($19 \text{ M}^{-1}\text{cm}^{-1}$) [43]. The efficiency of its photolysis
319 (equation 5, the final step for radical generation) has been reported to be considerably
320 impaired by the presence of pollutants found on wastewaters, especially for small
321 peroxide concentrations [43, 44]. The consequence is that, for stage 1, ozone is being
322 photolyzed (more ozone is being transferred) but less hydroxyl radicals are being formed.
323 Photolysis of ozone reduces the O_3 available for reactions of equations 1 and 2, thus
324 decreasing the hydroxyl radical production and the $R_{\text{OH}\cdot\text{O}_3}$ value in comparison to single
325 ozonation. In addition, there is possibly an overestimation of the initial rate of ACMP
326 degradation via direct photolysis, resulting in an underestimation of the total hydroxyl
327 radical exposure value (equation 12). The degradation rate of ACMP was obtained for
328 each matrix in a blank experiment without ozone flow, using only UV light. Since ozone
329 strongly absorbs UV at the 254 nm wavelength [45], less photons reached ACMP,
330 producing lower degradation by that route. During stage 2, the turbidity of the medium
331 and the ozone's reactivity with the matrices has been reduced. Consequently, more ozone
332 is available for photolysis, thus increasing peroxide formation and consequently $\cdot\text{OH}$
333 generation (equation 5 and 6). Stage 2 $R_{\text{OH}\cdot\text{O}_3}$ values for UV-C/ O_3 experiments were much
334 higher than in single ozonation for all wastewaters (80% for MBR, 51% for CAS-DN;
335 37% for CAS and 43% for MBBR) indicating the expected increase on hydroxyl radical
336 exposure per ozone consumed and the overall efficiency improvement of photolytic
337 ozonation.

338 When TiO_2 is added to ozonation, stage 2 $R_{\text{OH}\cdot\text{O}_3}$ values increased slightly for all
339 cases, while stage 1 value decreased for more polluted matrices CAS and MBBR. The

340 understanding of this is limited due to the lack of data regarding heterogeneous catalytic
341 ozonation performed in highly polluted wastewaters and the multiple interactions that
342 might be taking place between light, ozone, the catalyst and the matrix. However, possible
343 hypothesis is that the presence of TiO_2 may change the reactivity of molecular ozone with
344 the matrix, thus affecting the R_{OHO_3} value. Further studied should be performed in this
345 direction.

346 The effect of photocatalytic ozonation on R_{OHO_3} values was also much more
347 significant during second stage. Stage 2 R_{OHO_3} values for photocatalytic ozonation were
348 the highest of all assayed processes– which can be explained by the multiple radical
349 formation routes provided by the synergistic effect of ozonation and heterogeneous
350 photocatalysis combined [23]. Thus, stage 2 R_{OHO_3} values reached values higher than
351 double for all wastewaters, compared with single ozonation (105% increase in CAs-DN
352 and CAS; 121% increase in MBR and 127% increase in most polluted wastewater
353 MBBR). These values confirm the importance of phtotocatalytic process on promoting
354 the radical pathway in ozonation. On the other hand, stage 1 values for less turbid waters
355 MBR and CAS-DN were higher than on single ozonation, most probably due to the
356 smaller effect of organic matter and higher light absorption by TiO_2 .

357 Table 3 also shows the amount of TOD needed to reach 65% of ACMP
358 degradation for each process and matrix. As expected, less polluted matrices and light-
359 assisted ozonation processes attaining higher R_{OHO_3} needed less transferred ozone in
360 general to reach this degradation value.



361

362 Figure 2. $R_{\text{OH}\cdot}$ plots for all experiments. Gas flow rate = 0.3 L min^{-1} ; Inlet (g) ozone concentration = 10

363 mg O_3 L^{-1} ; $T_{\text{reaction}} = 20 \pm 2$ °C; $T_{\text{in}}(\text{gas}) = 22 \pm 2$ °C; $P_{\text{in}}(\text{gas}) = 25 \pm 2$ mbar.

364

365 The results confirm that $R_{\text{OH}\cdot}$ is an important parameter to determine the

366 availability of hydroxyl radical on each wastewater matrix, being useful to compare

367 radical production for each process and wastewater tested. It can also be used to predict

368 the amount of TOD required for degrading ozone-resistant micropollutants during

369 ozonation (equation 11) [35, 36]. Last assays were performed to evaluate the application
370 of 2 stage R_{OH,O_3} values of MBR effluent for the prediction of atrazine removal. This
371 pesticide presents low reactivity towards ozone, with second-order rate constant of 6 M^{-1}
372 s^{-1} and high reactivity with hydroxyl radicals ($k_{\bullet OH}$ of $3.0 \cdot 10^9 \text{ M}^{-1}\text{s}^{-1}$) [33]. Plots of the
373 predicted and experimental atrazine abatement in ozonation and photocatalytic ozonation
374 are presented in Figure S12. In both cases, a good agreement between model predictions
375 and experimental measurements was observed. Further experiments should be performed
376 with different micropollutants for its final validation.

377

378 **4. Conclusions**

379 In this work, UV light-assisted ozonation processes attained higher degradation
380 results of recalcitrant and ozone-resistant pesticide acetamiprid than single ozonation on
381 real domestic wastewaters.

382 More polluted matrices had higher ozone transfer yields due to their reactivity
383 with the oxidant. The presence of UV-C increased ozone consumption mass for all cases
384 due to ozone photolysis, while adding UV-A in the presence of TiO_2 increased ozone
385 consumption only for the less polluted matrices because they allowed a more efficient
386 photocatalytic activity.

387 The adaptation of the R_{OH,O_3} concept presented good fitting results for all
388 experiments, adopting ACMP as a probe compound. The plots had to be divided in two
389 stages, before and after the corresponding IOD, due to the initial presence of highly
390 reactive compounds towards molecular ozone in all wastewaters.

391 The improvement brought by both UV light-based processes on ACMP
392 degradation was directly related with the increase in stage two R_{OH,O_3} values in all

393 matrices. On that stage, photolytic ozonation values were up to 54% higher compared
394 with single ozonation while for photocatalytic ozonation values were higher than double
395 for all wastewaters studied (between 105 to 127%). These results demonstrate the
396 capacity of light assisted ozonation processes on the enhancement of radical pathway
397 degradation of ozone recalcitrant micropollutants, as well as the usefulness of modified
398 R_{OH/O_3} parameter on its quantification. To take advantage of the improvements in radical
399 production brought by UV light addition, the adoption of higher O_3 doses than the values
400 typically used for ozonation in WWTPs is required.

401

402 **5. Acknowledgments**

403 This Special Issue is dedicated to honor the retirement of Prof. César Pulgarin at
404 the Swiss Federal Institute of Technology (EPFL, Switzerland), a key figure in the area
405 of Catalytic Advanced Oxidation Processes. This work was financially supported by the
406 Spanish Ministry of Economy and Competitiveness (project CTQ2014-52607-R),
407 AGAUR - Generalitat de Catalunya (project 20145GR245). This work was funded by the
408 European Commission within the Erasmus+ KA1 Programme, Erasmus Mundus Joint
409 Master Degree in Chemical Innovation and Regulation.

410

411 **6. Bibliography**

412 [1] Y. Luo, W. Guo, H. Ngo, L. Nghiem, F. Hai, J. Zhang, S. Liang, W. Wang, A review
413 on the occurrence of micropollutants in the aquatic environment and their fate and
414 removal during wastewater treatment, *Sci. Total Environ.* 473-474 (2014) 619-641.
415 <https://doi.org/10.1016/j.scitotenv.2013.12.065>.

- 416 [2] M. Kim, K. Zoh, Occurrence and their removal of micropollutants in water
417 environments, Environ. Eng. Res. 21:4 (2016) 319-332.
418 <https://doi.org/10.4491/eer.2016.115>.
- 419 [3] S. Kurwadkar, X. Zhang, D. Ramirez, F. Mitchell, Emerging Micro-Pollutants in the
420 Environment: Occurrence, Fate, and Distribution, ACS Symposium Series (2015)
421 American Chemical Society: Washington, DC.
- 422 [4] B. Kasprzyk-Hordern, R. Dinsdale, A. Guwy, The Occurrence of Pharmaceuticals,
423 Personal Care Products, Endocrine Disruptors and Illicit Drugs in Surface Water in South
424 Wales, Water Res. 42:13 (2008) 3498-3518.
425 <https://doi.org/10.1016/j.watres.2008.04.026>.
- 426 [5] K. Fent, A.A. Weston, D. Carminada, Ecotoxicology of human pharmaceuticals,
427 Aquat. Toxicol. 76 (2006) 122-59. <https://doi.org/10.1016/j.aquatox.2005.09.009>
- 428 [6] A. Mecha, M. Onyango, M. Momba, Impact of ozonation in removing organic
429 micropollutants in primary and secondary municipal wastewater, Effect of processes
430 parameters. Water Sci. Technol. 74:3 (2016) 756-765.
431 <https://doi.org/10.2166/wst.2016.276>.
- 432 [7] J. Reungoat, B. Escher, M. Macova, F. Argaud, W. Gernjak, J. Keller, Ozonation and
433 biological activated carbon filtration of wastewater treatment plant effluents, Water Res.
434 46:3 (2012) 863-872. <https://doi.org/10.1016/j.watres.2011.11.064>.
- 435 [8] D. Gerrity, S. Gamage, J.C. Holady, D.B. Mawhinney, O. Quiñones, R.A. Trenholm,
436 S. Snyder, Pilot-scale evaluation of ozone and biological activated carbon 632 for trace
437 organic contaminant mitigation and disinfection, Water Res. 45 (2011) 2155-2165.
438 <https://doi.org/10.1016/j.watres.2010.12.031>.

439 [9] U. von Gunten, Ozonation of drinking water: Part I. Oxidation kinetics and product
440 formation, *Water Res.* 37 (2003) 1443-1467. [https://doi.org/10.1016/S0043-](https://doi.org/10.1016/S0043-1354(02)00457-8)
441 [1354\(02\)00457-8](https://doi.org/10.1016/S0043-1354(02)00457-8).

442 [10] M. Bourgin, B. Beck, M. Boehler, E. Borowska, J. Fleiner, E. Salhi, R. Teichler, U.
443 von Gunten, H. Siegrist, C.S. McArdell, Evaluation of a full-scale wastewater treatment
444 plant upgraded with ozonation and biological post-treatments: Abatement of
445 micropollutants, formation of transformation products and oxidation by-products, *Water*
446 *Res.* 129 (2018) 486-498. <https://doi.org/10.1016/J.WATRES.2017.10.036>.

447 [11] P. Stathatou, F. Gad, E. Kampfragou, H. Grigoropoulou, D. Assimacopoulos,
448 Treated Wastewater Reuse potential: mitigating water scarcity problems in the Aegean
449 Islands, *Desal. Water Treat. J.* 53:12 (2015) 3272-3282.
450 <https://doi.org/10.1080/19443994.2014.934108>

451 [12] F. Beltran, *Ozone Kinetics for Water and Wastewater systems*, CRC Press Lewis
452 Publishers, 2004, pp. 193-27.

453 [13] M. Dodd, M. Buffle, U. von Gunten, Oxidation of antibacterial molecules by aqueous
454 ozone: moiety-specific reaction kinetics and application to ozone-based wastewater
455 treatment, *Environ. Sci. Tech.* 40 (2006) 1969-1977. <https://doi.org/10.1021/es051369x>.

456 [14] G.V. Buxton, C.L. Greenstock, W.P. Helman, A.B. Ross, Critical Review of rate
457 constants for reactions of hydrated electrons, hydrogen atoms and hydroxyl radicals in
458 aqueous solution, *J. Phys. Chem. Ref. Data* 17 (1988) 513-886.
459 <https://doi.org/10.1063/1.555805>.

460 [15] NDRL/NIST Solution Kinetics Database. <http://kinetics.nist.gov/solution/>.
461 (accessed 22 April 2018).

- 462 [16] J. Yang, U. Wu, H. Tai, W. Sheng, Effectiveness of an ultraviolet-C disinfection
463 system for reduction of health-care associated pathogens, *J. Microbiol. Immunol. Infect.*
464 (2017). <https://doi.org/10.1016/j.jmii.2017.08.017>.
- 465 [17] S. Satyro, E. Saggiaro, F. Verissimo, D. Buss, D. Paiva Magalhaes, A. Oliveira,
466 Triclocarban: UV photolysis, wastewater disinfection and ecotoxicology assessment
467 using molecular biomarkers, *Environ. Sci. Pollut. Res. Int.* 24:19 (2017) 16077-16085.
468 <https://doi.org/10.1007/s11356-017-9165-4>.
- 469 [18] Z. Chen, J. Fang, C. Fan, S. Shang, Oxidative degradation of N-Nitrosopyrrolidine
470 by the ozone/UV process: Kinetics and pathways, *Chemosphere* 150 (2016) 731-739.
471 <https://doi.org/10.1016/j.chemosphere.2015.12.046>.
- 472 [19] D. Robert, R. Daghirt, P. Drogui, Modified TiO₂ For Environmental Photocatalytic
473 Applications: A Review, *Ind. Eng. Chem. Res.* 52:10 (2013) 3581-3599.
474 <https://doi.org/10.1021/ie303468t>.
- 475 [20] I. Ola, M. Maroto-Valer, Review of material design and reactor engineering on TiO₂
476 photocatalysis for CO₂ reduction, *J. Photochem. Photobiol. C- Photochem. Rev.* 24
477 (2015) 16-42. <https://doi.org/10.1016/j.jphotochemrev.2015.06.00>.
- 478 [21] J. Carbajo, A. Bahamonde, M. Faraldos, Photocatalyst performance in wastewater
479 treatment applications: Towards the role of TiO₂ properties. *Mol. Catal.* 434 (2017) 167-
480 174. <https://doi.org/10.1016/j.mcat.2017.03.018>.
- 481 [22] A. Lisenbigler, G. Lu, J. Yates, Photocatalysis on TiO₂ Surfaces: Principles,
482 Mechanisms, and Selected Results, *Chem. Rev.* 95 (1995) 735-758.
483 <https://doi.org/10.1021/cr00035a013>.

484 [23] Y. Guo, L. Yang, X. Cheng, X. Wang, The Application and Reaction Mechanism of
485 Catalytic Ozonation in Water Treatment, *J. Environ. Anal. Toxicol.* 2:150 (2012).
486 <https://doi.org/10.4172/2161-0525.1000150>.

487 [24] E. Emam, Effect of ozonation combined with heterogeneous catalysts and ultraviolet
488 radiation on recycling of gas-station wastewater, *Egypt. J. Petrol.* 21:1 (2012) 55-60.
489 <https://doi.org/10.1016/j.ejpe.2012.02.008>.

490 [25] K.P. Yu , G. Whei-May Lee, G.H. Huang, The Effect of Ozone on the Removal
491 Effectiveness of Photocatalysis on Indoor Gaseous Biogenic Volatile Organic
492 Compounds, *J. Air Waste Manag. Assoc.* 60:7 (201) 820-829.
493 <https://doi.org/10.3155/1047-3289.60.7.820>.

494 [26] F. Parrino, G. Camera-Roda, V. Loddo, G. Palmisano, V. Augugliaro, Combination
495 of ozonation and photocatalysis for purification of aqueous effluents containing formic
496 acid as probe pollutant and bromide ion, *Water Res.* 50 (2014) 189-199.
497 <https://doi.org/10.1016/j.watres.2013.12.001>.

498 [27] F. Beltran, A. Aguinaco, J. Garcia-Araya, Kinetic modelling of TOC removal in the
499 photocatalytic ozonation of diclofenac aqueous solutions *Appl. Catal. B: Environ.* 100:1-
500 2 (2010) 289-298. <https://doi.org/10.1016/j.apcatb.2010.08.005>.

501 [28] O. Eren, E. Kusvuran, A. Yildirim, S.A. Gul, Comparative Study of Ozonation,
502 Homogeneous Catalytic Ozonation, and Photocatalytic Ozonation for C.I. Reactive Red
503 194 Azo Dye Degradation, *Clean soil air water.* 39:8 (2011) 795-805.
504 <https://doi.org/10.1002/clen.201000192>.

505 [29] R. Rajeswari, S. Kanmani, Degradation of Pesticide by Photocatalytic Ozonation
506 Process and Study of Synergistic Effect by Comparison with Photocatalysis and

507 UV/Ozonation Processes, J. Adv. Oxid. Technol. 12:2 (2009) 208-214.
508 <https://doi.org/10.1515/jaots-2009-0209>.

509 [30] R. Solis, F. Rivas, J. Perez-Bote, O. Gimeno, Photocatalytic ozonation of 4-chloro-
510 2-methylphenoxyacetic acid and its reaction intermediate 4-chloro-2-methyl phenol, J.
511 Taiwan Inst. Chem. Engin. 46 (2015) 125-131.
512 <https://doi.org/10.1016/j.jtice.2014.09.010>.

513 [31] O. Gimeno, F. Rivas, F. Beltran, M. Carbajo, Photocatalytic Ozonation of Winery
514 Wastewaters, J.Agric. Food. Chem, 55:24 (2007) 9944-9950.
515 <https://doi.org/10.1021/jf072167i>.

516 [32] N. Moreira, J. Sousa, G. Macedo, A. Ribeiro, L. Barrieros, M. Pedrosa, J. Faria, M.
517 Pereira, S. Castro-Silva, M. Segundo, C. Manaia, O. Nunes, A. Silva, Photocatalytic
518 ozonation of urban wastewater and surface water using immobilized TiO₂ with LEDs:
519 Micropollutants, antibiotic resistance genes and estrogenic activity, Water Res. 94 (2016)
520 10-22. <https://doi.org/10.1016/j.watres.2016.02.003>.

521 [33] J. Acero, K. Stemmler, U. von Gunten, Degradation Kinetics of Atrazine and its
522 degradation products with ozone and OH radicals: a predictive tool for drinking water
523 treatment, Environmental Sci. Tech. 34 (2000) 591-597.
524 <https://doi.org/10.1021/es990724e>.

525 [34] M.S. Elovitz, U. von Gunten, Hydroxyl Radical/ Ozone Ratios During Ozonation
526 Processes. I. The Rct Concept, Ozone Sci. Eng. 21:3 (1999) 239-260.
527 <https://doi.org/10.1080/0191951990854723>.

528 [35] M. Kwon, H. Kye, Y. Jung, Y. Yoon, H. Kang, Performance characterization and
529 kinetic modeling of ozonation using a new method: R_{OH}O₃ concept, Water Res. 122 (2017)
530 p 172-182. <https://doi.org/10.1016/j.watres.2017.05.062>.

531 [36] A. Cruz-Alcalde, S. Esplugas, C. Sans, Abatement of ozone-recalcitrant
532 micropollutants during municipal wastewater ozonation: kinetic modelling and surrogate-
533 based control strategies, Chem. Eng. J. In press.
534 <https://doi.org/10.1016/j.cej.2018.10.206>.

535 [37] S. Canonica, L. Meunier, U. von Gunten, Phototransformation of selected
536 pharmaceuticals during UV treatment of drinking water, Water Res. 42 (2008) 121-128.
537 <https://doi.org/10.1016/j.watres.2007.07.026>.

538 [38] M. Marce, B. Domenjoud, S. Esplugas, S. Baig, Ozonation treatment of urban
539 primary and biotreated wastewaters: Impacts and modeling, Chem. Eng. J. 283 (2016)
540 768-777. <https://doi.org/10.1016/j.cej.2015.07.073>.

541 [39] A. Cruz-Alcalde, C. Sans, S. Esplugas, Priority pesticide abatement by advanced
542 water technologies: the case of acetamiprid removal by ozonation, Sci, Total Environ.
543 599-600 (2017) 1454-1461. <http://dx.doi.org/10.1016/j.scitotenv.2017.05.065>.

544 [40] D. Gardoni, R. Canziani, Decay of ozone in water: a review, Ozone Sci. Eng. 34:4
545 (2012) 233-242. <https://doi.org/10.1080/01919512.2012.686354>.

546 [41] A. Yavas, Catalytic ozonation of paracetamol using commercial and Pt-supported
547 nanocomposites of Al₂O₃: The impact of ultrasound, Ultrason. Sonochem. 40 (2018) 175-
548 182. <https://doi.org/10.1016/j.ultsonch.2017.02.017>.

549 [42] R. Zhang, D. Yuan, B. Liu, Kinetics and products of ozonation of C.I. Reactive Red
550 195 in semi-batch reactor, Chin. Chem. Lett. 26:1 (2015) 93-
551 99. <https://doi.org/10.1016/j.ccllet.2014.10.024>.

552 [43] W. Audenaert, Y. Vermeersch, Y. Van Hulle, P. Dejans, A. Dumoulin, I. Nopens,
553 Application of a mechanistic UV/hydrogen peroxide model at full scale: sensitivity

554 analysis, calibration and performance evaluation, Chem. Eng. J. 171:1 (2011) 113-126.
555 <https://doi.org/10.1016/j.cej.2011.03.071>.

556 [44] P. Andersen, C. Williford, J. Birks, Miniature personal ozone monitor based on UV
557 Absorbance, Anal. Chem. 82:19 (2010) 7924-7928. <https://doi.org/10.1021/ac1013578>.

558 [45] S. Gora, S. Andrews, Adsorption of natural organic matter and disinfection
559 byproduct precursors from surface water onto TiO₂ nanoparticles: pH effects, isotherm
560 modelling and implications for using TiO₂ for drinking water treatment, Chemosphere
561 174 (2017) 363-370. <https://doi.org/10.1016/j.chemosphere.2017.01.125>.

562

563

564